

Anke M. van Mourik · Andreas Daffertshofer
Peter J. Beek

Deterministic and stochastic features of rhythmic human movement

Received: 3 July 2005 / Accepted: 21 November 2005 / Published online: 28 December 2005
© Springer-Verlag 2005

Abstract The dynamics of rhythmic movement has both deterministic and stochastic features. We advocate a recently established analysis method that allows for an unbiased identification of both types of system components. The deterministic components are revealed in terms of drift coefficients and vector fields, while the stochastic components are assessed in terms of diffusion coefficients and ellipse fields. The general principles of the procedure and its application are explained and illustrated using simulated data from known dynamical systems. Subsequently, we exemplify the method's merits in extracting deterministic and stochastic aspects of various instances of rhythmic movement, including tapping, wrist cycling and forearm oscillations. In particular, it is shown how the extracted numerical forms can be analysed to gain insight into the dependence of dynamical properties on experimental conditions.

1 Introduction

The quest for an adequate mathematical framework for describing motor behaviour has a long and checkered tradition in human movement science. Most efforts to date have focussed on recurrent, deterministic features of behaviour although studies accentuating variable or stochastic aspects of human movement are on the rise. In spite of this development the deterministic and stochastic features of human movement are seldom assessed in conjunction. In the present paper, we describe a recently established analysis method that allows for the unbiased specification of deterministic and stochastic system components. After a brief general summary of this method, we explore its expediency in analyzing kinematic

data that were collected during different instances of rhythmic movement. The ultimate goal of this analysis is to find mathematical descriptions that exhibit the main dynamic features of the system under study. In order to illustrate which features need to be covered and the merits of the advocated approach, we shall first discuss the limitations of the methods that have been used in recent years in the context of modelling rhythmic movements in terms of self-sustaining oscillations or limit cycles, either with or without noise. Invariably, these more conventional methods are based on a priori assumptions regarding the analytical form of the dynamics and incorporation of the system's stochasticity.

The use of dynamical systems to account for the qualitative features of end-effector trajectories of limb oscillations gained momentum in the last two decades. In this approach salient characteristics of human movement typically served as guidelines for model development. For instance, trajectories of limb cycling describe a bounded area in the position-velocity or phase plane may be interpreted as indicative of a limit cycle attractor, at least when modelling efforts are restricted to identifying deterministic forms, thereby disregarding variability.

Using averaging methods from the theory of nonlinear oscillators, such as the slowly-varying amplitude approximation and harmonic balance analysis, Kay et al. (1987, 1991) derived second-order nonlinear differential equations that mimicked experimentally observed amplitude-frequency relation and the phase response characteristics of rhythmic finger and wrist movements. In particular, these self-sustaining oscillators included weak dissipative nonlinearities that stabilized the limit cycle and caused a drop of amplitude (accounted for by a Rayleigh term) and an increase in peak velocity (accounted for by a van der Pol term) with increasing movement tempo (i.e., frequency). Building on normal form theory but aiming at a broader applicability, Beek and Beek (1988) devised a generic method for determining, from any given oscillatory trajectory, the (minimal) nonlinear components and accompanying coefficients required for reproducing that trajectory. Beek and Beek (1988) assumed that rhythmic limb movements could be formulated

A.M. van Mourik (✉) · A. Daffertshofer · P.J. Beek
Institute for Fundamental and Clinical Human Movement Sciences,
Vrije Universiteit, Van der Boechorststraat 9, 1081BT Amsterdam,
The Netherlands
E-mail: a.vanmourik@fbw.vu.nl
Tel.: +31-20-5988507
Fax: +31-20-5988529

as second-order dynamics based on an ideal mass-spring system with additional nonlinear (polynomial) components (dissipative or damping and conservative or stiffness terms), summarized as the so-called *W*-function. They showed how parameter values reflecting the strength of their corresponding terms could be estimated graphically by plotting measured time series against conveniently chosen functional forms to test the presence of particular polynomial terms. A more rigorous way to compute parameter values is to regress all state variables (e.g., position and velocity) onto the analytical form of the *W*-function. Apart from the aforementioned combination of Rayleigh and van der Pol oscillators, this regression yielded Duffing-like cubic stiffness for swinging a hand-held pendulum at a given frequency and amplitude (Beek et al. 1995). In a similar fashion but circumventing collinearity problems in the proposed regression technique, Bootsma et al. (1998) and Mottet and Bootsma (1999) studied the dynamics of goal-directed rhythmic aiming movements in the context of a cyclical Fitts' task. Using Beek and Beek's (1988) graphical analysis, they identified and then incorporated Duffing and Rayleigh components, although under specific task constraints the introduction of additional dynamical components proved necessary. Preserving system symmetry, Mottet and Bootsma (1999) suggested the presence of a quintic stiffness term to account for possible overshoots and a cubic van der Pol term to stabilize the oscillations for tasks with a low index of difficulty, i.e., relatively easy tasks. Eisenhammer et al. (1991) introduced an approach for extracting ordinary differential equations from experimental time series similar to that proposed by Beek and Beek (1988), except that in their method the experimental data are represented in a state space and the corresponding flow vectors are approximated by polynomials of the state vector components. Using this method, they obtained, for a single oscillating limb, excellent agreement between the limit cycle displayed by the experimental system and the reconstructed model, in spite of the noisiness of the data (see also Perona et al. 2000, for review). For systems of two coupled limit cycle oscillators, however, reconstruction was only successful for data with a sufficiently long transient trajectory and a relatively low noise level. The cyclical movements studied in the aforementioned studies were rather similar and so were the identified models. Note, however, that the limited spectrum of polynomial forms of all the listed models reflects a crucial a priori assumption: number and form of the polynomial coefficients are chosen by the modeler. The fair diversity of model parameters, however, already demonstrates that appropriate mathematical descriptions of rhythmic motor behaviour may be at variance. Put differently, all of the the summarized approaches consider certain analytical forms of the to-be-determined dynamics. Hence, the model output (i.e., simulated movement trajectories) can be prescribed by choosing certain parameter combinations that are obtained through optimal matches between model and data, relying on the assumption that differences in parameters reflect differences in tasks or task constraints. The approaches further have in common that they focus on pre-

dictable (deterministic) elements of human movement. The stochastic properties of limb oscillations, although explicitly acknowledged by at least some authors in this context (e.g., Eisenhammer et al. 1991; Kay 1988), are usually considered noise that obscures the deterministic dynamics and thus should be eliminated by means of filtering or averaging.

Recently, there has been an upsurge of studies focussing on stochasticity as a hallmark property of human movement that not only needs to be addressed, but also possesses functional qualities (e.g., Harris and Wolpert 1998; Körding and Wolpert 2004; Riley and Turvey, 2002; Schöner et al. 1986; Schöner 2002). For instance, variability in endpoint trajectory has been associated with task difficulty (Todorov and Jordan 2002): variability is reduced in more difficult tasks to comply with accuracy constraints, whereas in easier tasks the variability is allowed to increase to enhance system flexibility. Another example of the usefulness of motor variability can be found in studies of interlimb coordination conducted from a dynamical systems perspective. In this context, variability has been incorporated as random fluctuations to account for phenomena like critical fluctuations and critical slowing down in the vicinity of phase transitions, that is, situations in which a system switches between stable states or attractors, e.g., switches from antiphase to in-phase coordination (Haken et al. 1985; Kelso 1984; Post et al. 2000; Schöner et al. 1986). In relation to the attractor strength, the amount of random fluctuations competes with stability and, thus, determines the flexibility of the system. That is, strong fluctuations reflect less stable states between which the system may readily switch, whereas weaker fluctuations indicate more stable states that can be steadily maintained. Formally, variability may be accounted for by incorporating either additive or multiplicative random fluctuations yielding stochastic differential equations. Schöner et al. (1986) and Schöner (1990) formulated stochastic models for single- and multi-limb movements similar to the abovementioned 'deterministic' limit cycle models (comprising van der Pol, Duffing and quintic stiffness terms) under the impact of stochastic forces (Gaussian white noise). Schöner (1990) also suggested similar accounts of discrete movement and postural sway, albeit without providing any empirical support. In recent years, a plenitude of experimental studies has appeared concerning the variable nature of human movement and posture (for a recent review see, e.g., Riley and Turvey 2002). Most of these studies are attempts to uncover the essence of noise by purely statistical means, although more recently suggestions have been made to incorporate variability within the description of movement via dynamical systems (e.g., Frank et al. 2001). From these examples it is evident that, analogous to the search for adequate analytical forms in the case of deterministic structures, no consensus has yet been reached regarding the precise mathematical implementation of variability or stochasticity.

The extraction procedure presented here allows for a direct assessment and evaluation of the deterministic and stochastic parts of an experimental system of interest as represented by empirical data. Thus, the method may render

an objective analysis tool that is, in principle, independent of a priori assumptions regarding the analytical form of the underlying dynamics. Possible changes of the dynamic structure due to altered experimental circumstances can be pinpointed by analyzing the extracted dynamics in its corresponding phase space. In the present study, this procedure will be explained in more detail and illustrated using both numerically simulated time series and experimentally obtained human movement data (finger tapping, wrist and forearm cycling).

2 Extraction procedure

Since its introduction (Friedrich and Peinke 1997), the extraction procedure has found application in physics (e.g., Friedrich and Peinke 1997; Waechter et al. 2003), engineering (Gradisek et al. 2000, 2002b), economics (Friedrich et al. 1997), sociology (Kriso et al. 2002) and meteorology (Sura 2003). The method has been successfully tested by analyzing simulated data from known dynamical systems such as nonlinear oscillators and chaotic systems (see, e.g., Gradisek et al. 2000; 2002a, 2002b; Siegert et al. 1998). Friedrich et al. (2000) introduced the method in the biological domain by investigating different types of tremor, while Kuusela et al. (2003) presented analyses of heart-rate fluctuations in humans suggesting new diagnostic tools. Before discussing its application in the study of human movement, we outline the method's fundamental principles, discuss its mathematical details and provide an analytical example.

2.1 General principles

Stochastic behaviour can be considered as the time evolution of a process under the impact of random fluctuations. By definition, the future states of a stochastic process cannot be predicted unambiguously from its present state. Any prediction is conditional upon the probability that a certain future state will occur, that is, to find the system's state at a certain instant in time in a specific area in state space. A collection of such probabilities indicating the likelihood of the occurrence of specific states is called a probability distribution function. The distribution function can be characterized by various statistical quantities such as its moments or cumulants. In combination, these properties provide a compact description of the stochastic process of interest. The first cumulant is the mean, the second the variance, the third the skewness of the distribution (or the process), and so on. For example, a normal, or Gaussian, distribution describes the probability of finding a single system in a specific state and is solely specified by its mean and standard deviation (i.e., square root of the variance). For the general mathematical framework considered here, however, probability depends on state space location as well as on time so that, in order to describe both the probability distribution and its cumulants a (virtual) ensemble of systems is required, implying that,

e.g., mean and variance are computed over an ensemble of systems rather than over the evolution of a single system. Put differently, the probability distribution is given via a distribution of a (virtual) collection of identical systems that intermingle as the result of their spontaneous evolution influenced by random fluctuations. If the process is diffusive, then the first two cumulants determine the dynamics of the probability distribution while higher cumulants are irrelevant (i.e., there are no jumps in the evolution of the probability distribution, see, e.g., Honerkamp 1998, chapter 5.6). Also human movement may be characterized as (the result of) a diffusion process, because it can often be captured in the form of common stochastic differential equations, that is, a dynamical system (or differential forms) comprising both deterministic and stochastic components. The unique link between these deterministic and stochastic components and the first two cumulants of the corresponding probability distribution is well documented (Gardiner 2004; Kramers 1940; Moyal 1949; Risken 1989; Stratonovich 1963) and has provided a theoretical framework for understanding the interaction between deterministic and random features (Haken 1983).

2.2 Notation and forms

The extraction of the deterministic and stochastic components is based on the calculation of probability distributions. Since we view human movement as a deterministic system with noise that obeys (a system of) stochastic differential equation(s), the time evolution of the corresponding probability distribution can be described by an equation of motion, which in general may be written in the form:

$$\frac{d}{dt}P(x, t) = L_{FP}P(x, t), \quad (1)$$

where $P(x, t)$ denotes the probability distribution, i.e., $\int_x^{x+dx} P(x', t)dx'$ is the probability of finding the system's state at time t in the interval $[x, x + dx]$, and L_{FP} refers to an arbitrary form (operator) that may also depend on space and time. Suppose we have a diffusion process that can be expressed in the form of the so-called generalized Langevin equation:

$$\dot{\xi} = f(\xi) + g(\xi)\Gamma[t], \quad (2)$$

$\xi = \xi(t)$ denotes some arbitrary function describing the system's present state, with the dot-notation $\dot{\xi}$ indicating differentiation with respect to time.¹ The functions f and g represent the deterministic and stochastic components of the system, respectively. That is, f combines all deterministic forces acting on ξ , and g represents possible state dependent

¹ In accounting for (bio)mechanical features of human movement, typically second-order deterministic dynamical systems that include inertia are exploited (that may yield nonlinear oscillators like the ones discussed in, e.g., Beek et al. 1996; Haken et al. 1985; Kay et al. 1987; Mottet and Bootsma 1999; Schöner et al. 1986). For the sake of simplicity, however, we will explain the basic mathematical features in one dimension and refer to Appendix A for further details on multidimensional systems.

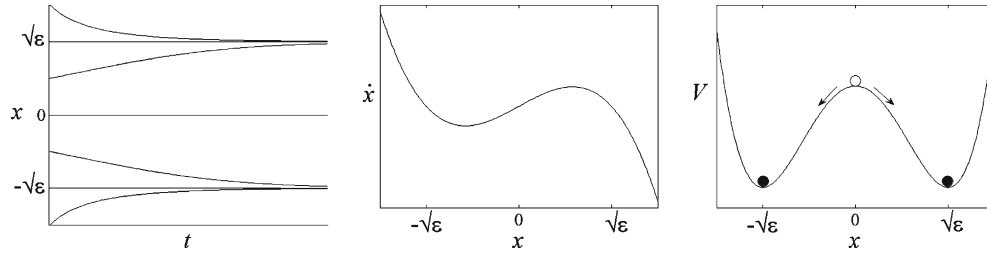


Fig. 1 $\epsilon > 0$, *Left* Time series of variable x as generated with Eq. (8) for different initial conditions. *Middle* deterministic component of (8). *Right* potential function V ; the stable states are indicated by the black ‘balls’ at the bottom of the ‘wells’, the unstable state is represented by the white ‘ball’ on top of the ‘hill’

forms that modulate random fluctuations $\Gamma [t]$ before being incorporated into the system’s dynamics.² The numerical representations of the functions f and g are the central quantities of the method discussed here as they represent the values to be extracted. For the moment we restrict the extraction to autonomous systems for which f and g depend explicitly on the state variable but not on time, that is, we consider time-invariant deterministic and stochastic components. For a Langevin Eq. (2) the form L_{FP} in Eq. (1) readily becomes:

$$L_{FP} = -\frac{\partial}{\partial x} \left\{ D^{(1)}(x) - \frac{\partial}{\partial x} D^{(2)}(x) \right\} \quad (3)$$

This yields a diffusion equation, the so-called Fokker–Planck equation:

$$\frac{\partial}{\partial t} P(x, t) = -\frac{\partial}{\partial x} \left\{ D^{(1)}(x) - \frac{\partial}{\partial x} D^{(2)}(x) \right\} P(x, t), \quad (4)$$

$D^{(1)}(x)$ and $D^{(2)}(x)$ are identified as drift and diffusion coefficients, respectively. Specifically, the deterministic and stochastic parts f and g of the Langevin equation (2) are related to the drift and diffusion coefficients $D^{(1)}(x)$ and $D^{(2)}(x)$ in the Fokker–Planck equation (4) by means of:

$$f(x) = D^{(1)}(x) \quad \text{and} \quad g(x) = \sqrt{2D^{(2)}(x)}. \quad (5)$$

Hence, the original Langevin equation can be rewritten as:

$$\frac{d}{dt} \xi = D^{(1)}(\xi) + \sqrt{2D^{(2)}(\xi)} \Gamma [t] \quad (6)$$

and the drift coefficient corresponds to the deterministic part of the dynamical equations, whereas the diffusion coefficient is related to the noise. The drift and diffusion coefficients are identical to the first- and second-order cumulants or the first two Kramers–Moyal coefficients of the conditional probability distribution. A cumulant of an arbitrary order n (or the n th order Kramers–Moyal coefficients) can be computed as:

$$D^{(n)}(x) = \lim_{\tau \rightarrow 0} \frac{1}{\tau} \int \frac{[x' - x]^n}{n!} P(x', t + \tau | x, t) dx', \quad (7)$$

where τ represents an infinitesimal time step as the limit approaches zero. The conditional probability distribution $P(x', t' | x, t)$ represents the probability of the system to be

found in state x' at time $t + \tau$, given a previous state x at time t . Once this probability is computed on the basis of experimental data, Eq. (7) can be used to determine the drift and diffusion coefficients.

Importantly, before applying this extraction procedure, the general description in terms of stochastic dynamics given by Eq. (2) needs to be validated. To this end, one has to verify whether the system under study can be described as a Markov process, that is, as a system whose future probability density depends only on its present value and not on its history (see Appendix B for a more detailed account). To exploit Eq. (7), the data have to be binned, that is, the range of values of each variable has to be subdivided into equally spaced parts or bins. Every bin is represented by the coordinate(s) specifying its centre. Subsequently, the conditional probability density distribution $P(x', t' | x, t)$ can be determined by computing the probability to find a sample at time t' in a bin with centre x' assuming that at time t the previous sample was found in a bin with centre x (note that $t' > t$). This computation has to be carried out for all neighbouring pairs of samples and all combinations of bins. According to (7), the resulting values of the conditional probability density distribution are multiplied by their corresponding differences (raised to the power n) so that integration over the bins of the ‘next’ sample and scaling by the time step yields drift and diffusion coefficients.

2.3 An analytical example

To demonstrate the outlined mathematical procedure in practice we consider a dynamical system with a cubic nonlinearity. In its deterministic form, the dynamics reads:³

$$\dot{x} = \epsilon x - x^3 = -\frac{dV}{dx} \quad \text{with} \quad V(x) = -\frac{\epsilon}{2}x^2 + \frac{1}{4}x^4, \quad (8)$$

$V = V(x)$ represents the potential function. For $\epsilon > 0$, this system has three stationary states, i.e., $x = x_0 = 0$ as unstable fixed point and $x_{1,2} = \pm\sqrt{\epsilon}$ as stable ones (see Fig. 1).

By adding white noise, system (8) becomes a stochastic dynamics of the form:

$$x \rightarrow \xi : \quad \dot{\xi} = \epsilon \xi - \xi^3 + \sqrt{2Q} \Gamma_t. \quad (9)$$

² $\Gamma_i [t]$ denote independent Gaussian white noise sources with uncorrelated mean, that is, $\langle \Gamma_i [t] \rangle = 0$, $\langle \Gamma_i [t] \Gamma_j [t'] \rangle = \delta_{ij} \delta(t - t')$.

³ The system allows for a supercritical pitchfork bifurcation with bifurcation parameter ϵ .

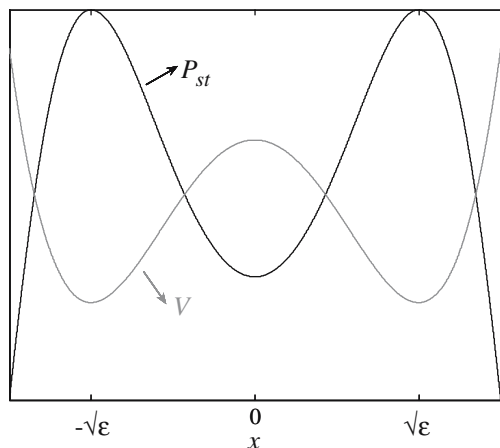


Fig. 2 Sketch of the probability distribution P_{st} , and the potential function V

In view of (4) the corresponding Fokker–Planck equation can be written as:

$$\frac{\partial P}{\partial t} = -\frac{\partial}{\partial x} \left(\epsilon x - x^3 - Q \frac{\partial}{\partial x} \right) P. \quad (10)$$

Importantly, one can explicitly compute the stationary solution of (10) by substituting $P = P_{st} = P_{st}(x)$ or $\partial P_{st}/\partial t = 0$ yielding $P_{st} \propto e^{-(V/Q)}$. Given stationarity, P_{st} represents the distribution of the probability to find the system in an interval $[x, x + dx]$ (Fig. 2).

To illustrate the corresponding extraction of drift and diffusion coefficients, we simulated a time series via the numerical form of Eq. (9) yielding 10^6 data samples (see Fig. 3, left panel). Figure 3 (middle and right panel) shows the numerical values for both the extracted deterministic component and its potential function. As can be appreciated from these figures, the extracted dynamics match the original analytical function very well.

2.4 Short data and averaging

The quality of the extracted dynamics critically depends on the quality of the computed transition probabilities. As is commonly the case in statistical approaches, the number of available data points is a vital factor because it determines the quality of the estimates. As we need to determine transition probabilities, data points should be collected in a single recording as this may guarantee that transition rates are constant (stationary case). In studies of phenomena such as turbulence (for which the approach was originally formulated), collecting large numbers of data is, in principle, only limited by external factors like computer capacity and the experimenter’s patience. In biology, in contrast, the system itself readily provides boundaries to data collection just by virtue of its finite life span. Besides such theoretical issues, more practical concerns arise when studying human movement. For instance, a participant can only perform so many voluntary finger oscillations before fatigue sets in. Whenever

this is the case, the dynamical process under study may no longer be stationary and another time scale may become relevant. The most common way to avoid such effects is to collate data recorded during multiple trials. Accordingly, when estimating transition probabilities we apply the following averaging procedure: (a) compute the transition probability $P(x', t'|x, t)$ per individual trial;⁴ (b) average these transition probabilities to obtain a representative transition probability for the entire experimental set; (c) use the mean probability in Eq. (7); in doing so we assume statistical independence of trials and time invariance of the underlying dynamics across recordings. The numerical estimates turn out to be rather robust against different ways of data collection (single long recording versus multiple short recordings) while the accuracy of the estimate is related to the total number of data points (see van Mourik et al. 2005, in press).

3 Application to human movement

While the analytical example in the previous section served to illustrate the essence of the extraction procedure, we have yet to demonstrate the merits of the approach in studying human movement. With this aim, we apply the procedure to experimentally obtained kinematic data. Three types of unimanual cyclic movement data will be used for this purpose: forearm oscillations (van den Berg et al. 2000), wrist cycling and finger tapping (Beek et al. 2002). The unique qualities of each of these instances of rhythmic movement will allow us to highlight several aspects of the method’s potential in analyzing human movement. As the data sets in question have already been published, we can keep the description of the respective experimental procedures to a minimum and show extensively how to apply the extraction method and interpret its results. In addition to visualization techniques for drift and diffusion coefficients, methods for direct comparison and obtaining analytical forms will be discussed.

3.1 Experimental settings: data collection and pre-processing

The forearm cycling data were collected in an experiment involving 16 healthy subjects. In addition to an unpaced condition, there were paced conditions in which the movements were paced with an auditory metronome at six different frequencies (0.5–3.0 Hz in steps of 0.5 Hz). Each condition was repeated four times and every trial comprised 30 cycles. The sample frequency was 500 Hz – see van den Berg et al. (2000) for further details regarding the experimental set-up. The wrist cycling and tapping data were collected in another experiment in which eight healthy subjects participated. A pacing signal was imposed for the first 25 cycles, after which the participants had to continue oscillating at the same rate for 35 more cycles. There were seven different pacing conditions (1.5–3.0 Hz in steps of 0.25 Hz) and each condition

⁴ Bins must match across trials.

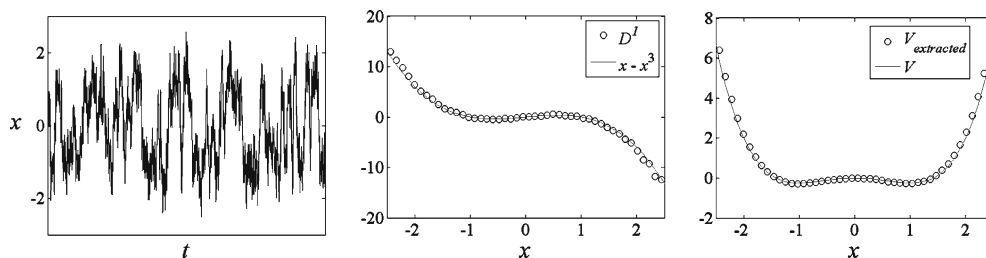


Fig. 3 *Left panel* Part of the time series simulated via Eq. (9) with $Q = 1$ and time step of 0.01. *Middle panel*: Circles Deterministic component of Eq. (9) obtained from the simulated time series via the extraction procedure. Line Original analytical function. *Right panel*: Circles Potential function (9) obtained from the simulated time series via the extraction procedure and subsequent integration. Line Original analytical potential function

was repeated six times. Sampling frequencies were 333 and 313 Hz for wrist cycling and finger tapping, respectively – see van Beers et al. (2002) for more details. The synchronization and continuation parts of the data were analysed separately.

In contrast to the analytical example we here account for the periodicity of the movements by assuming that the dynamical system underlying the data sets is two-dimensional: position and velocity are chosen as the relevant state variables.⁵ Unless stated otherwise, time series of both components were shifted in order to eliminate possible dc-components and, subsequently, individually rescaled to unit variance – note that rescaling eliminates conceivable changes in peak velocity, e.g., due to movement tempo. Furthermore, to avoid possible influences of trial length we re-sampled the data, thus guaranteeing equal numbers of samples in all conditions (equivalent to the number of samples in the longest trial). Prior to extracting drift and diffusion coefficients, we verified that the data exhibited Markov properties using the Chapman–Kolmogorov equation (see Appendix B).

3.2 Vector fields

The three data sets were analysed and individual results were averaged over repetitions per experimental condition. The extracted deterministic component consisted of two matrices, containing the numerical values of one of the two dynamical equations as a function of the location in phase space (i.e., in this case, the position-velocity or phase plane) each. These values might be interpreted as the components of vectors in phase space. As such, they were used to reconstruct a vector field to signify the data, i.e., creating a detailed phase space representation of the deterministic component. In Fig. 4 vector fields are depicted using the rescaled position but non-rescaled velocity data of forearm cycling at different pacing frequencies. General features of self-sustaining limit cycles, like a steady amplitude that decreases with increasing frequency can be observed (note that the amplitude is fixed here so that, in relative terms, velocity increases).

3.3 Direct comparison: difference fields

Rescaling both variables to unit variance allows for a direct comparison of vector fields that are extracted from data obtained under different experimental conditions. Figure 5 shows detailed differences between limit cycle attractors of forearm cycling at different movement tempos and between paced and unpaced movements. For the latter the uniformity of the difference field indicates that the underlying attractors only differ in strength while slow and fast forearm cycling display local discrepancies, in particular during the acceleration and deceleration phase of the movement.

Besides changes in trajectories as a function of task conditions, different movement types can be analysed by looking at the corresponding difference fields (see Fig. 5b). For instance, when comparing tapping to wrist cycling, large differences are observed in the deceleration phase of the

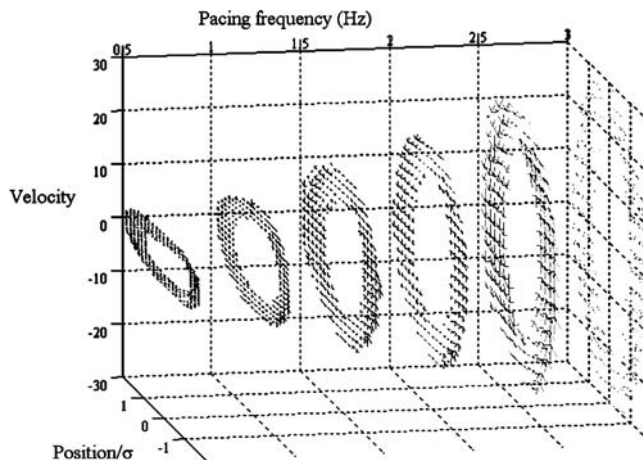


Fig. 4 Forearm cycling vector fields at different pacing frequencies. The increase of (peak) velocity with increasing movement frequency is clearly visible because velocity was not rescaled to unit variance. In general, a dynamics can only be reconstructed in phase space regions where data are actually present. This explains the limited regions in which the vector fields are displayed. The total number of samples in the time series bounds the (spatial) resolution of the estimates, i.e., the number of bins in the figure. As a consequence, the vector field resolution decreases with increasing movement frequency due to the accompanying increase of the vector field range and the fixed number of bins

⁵ We numerically estimated velocity after smoothing the position data via a polynomial filter (fifth-order Savitzky-Golay, frame size 35; Press et al. 1994)

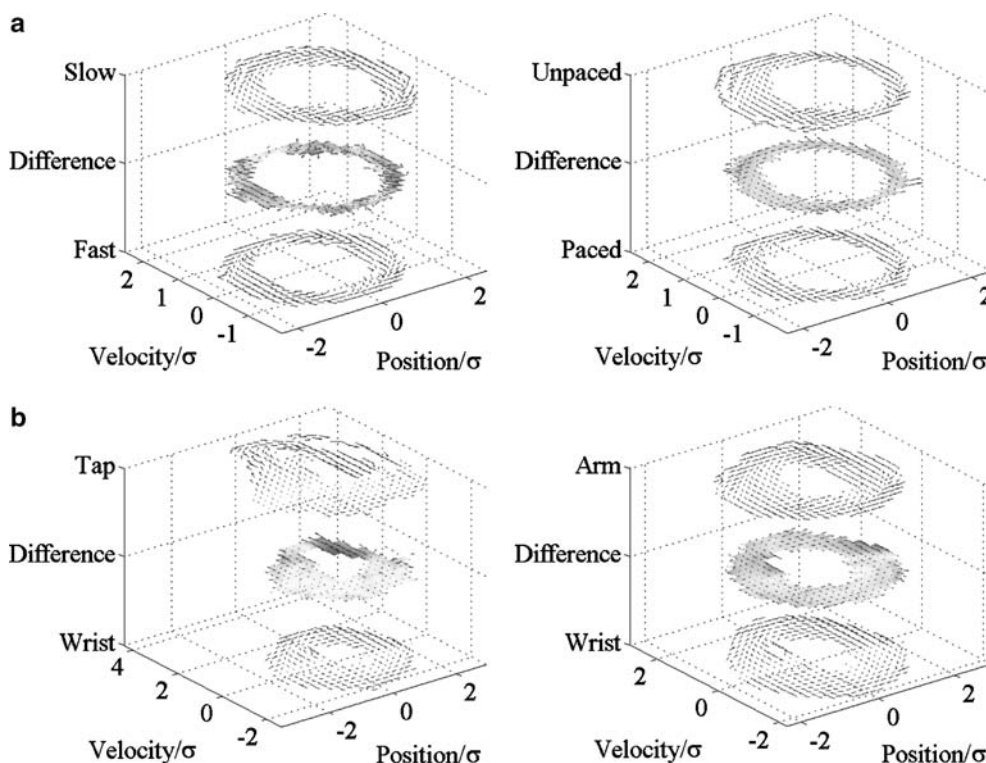


Fig. 5 **a** Difference fields for comparing slow (0.5 Hz) and fast (3.0 Hz) movements (*Left*) and unpaced versus paced (1 Hz) movements (*Right*). The upper and lower fields represent the to-be-compared conditions, while the centre field depicts the difference between these two vector field representations. The *darkness of the grey shading* corresponds to the length of the difference vectors and can be used to assess the size distribution of the difference field. These graphs contain forearm cycling data from a single participant. **b** Difference fields for comparing tapping and wrist cycling movements (1.5 Hz, *left panel*) and arm versus wrist cycling movements (1.5 Hz, *right panel*)

flexion movement. Although this observation may seem somewhat trivial from a mechanical point of view, because it can easily be explained by the fact that in tapping, in contrast to wrist cycling, a surface is hit, thereby clearly altering that phase of the movement, it is important to keep in mind that the analyses described in this section are meant as illustrations. Looking at arm cycling versus wrist cycling, the corresponding vector fields differ primarily in the vicinity of extreme positions (mainly in flexion): in wrist cycling anchor points are present that are less pronounced (or even absent) in the arm movements.

3.4 Phase portraits

The numerical forms of the dynamical equations (first Kramers–Moyal coefficient) can be utilised to generate time series. In combination with the reconstructed vector field the resulting phase portrait can provide a good impression of the system’s dynamics in the absence of noise. Figure 6a depicts the reconstructed deterministic dynamics for forearm cycling, wrist cycling and tapping, respectively. At the left-hand side the vector field is broader for all three movements because the underlying (recorded) trajectories were more variable in these regions. The maximum velocity also appears to be higher for flexion than extension movements.

Comparing the three graphs, the data are clearly governed by limit cycle attractors of different shapes. Further, anchoring is most pronounced in tapping: the different sizes of the vectors indicate a difference in the flow through the vector field, thereby visualizing a tendency to linger at the extreme positions.

3.5 Analytical estimates

So far, we have abstained from specifying the analytical form of the extracted dynamical equations because even without such a specification the analysis proposed here allows for qualitative interpretation of the system’s dynamics. In order to compare our results with the models in the literature we now investigate possible analytical forms of generating self-sustaining oscillators. Note that we determine the dynamics’ functional form after the previously explained extraction. That is, in principle, there are no restrictions to the explicit analytical form of the dynamics but in view of the models referred to in the introduction and the objective to account for the aforementioned more qualitative results, we here discuss polynomials up to the third order. For the sake of simplicity we initially limit the polynomials to odd nonlinearities: Eq. (9) was fitted to the three types of data shown in Fig. 6a; here, x refers to the recorded position and y to the corresponding velocity

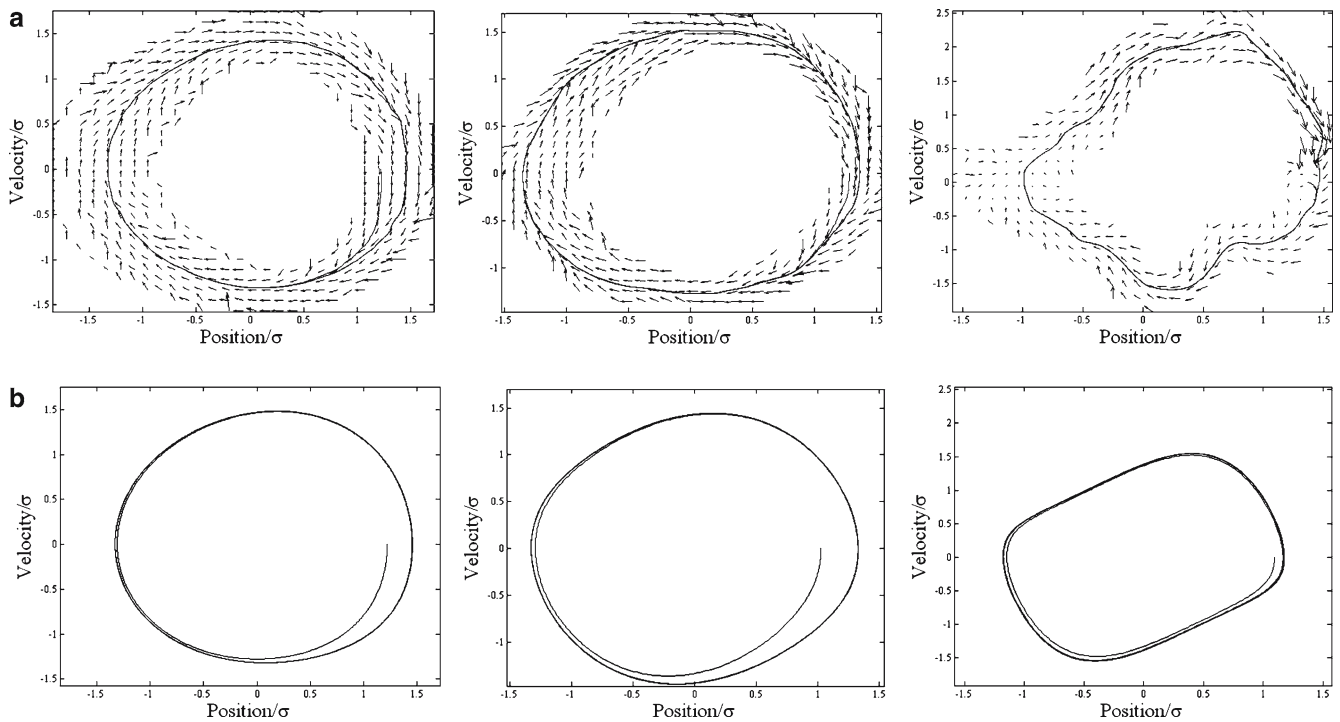


Fig. 6 **a** Reconstructed vector fields and phase portraits for tapping (*left panel*), wrist cycling (*middle panel*) and forearm cycling (*right panel*). The pacing frequency is 1.5 Hz in all three cases. Note that for tapping both the upper and lower halves (i.e., flexion vs. extension) and their right and left halves (i.e., acceleration vs. deceleration) are markedly different from each other. **b** Phase portraits generated by fitted function (Eq. 9) of forearm cycling (*left panel*), wrist cycling (*middle panel*) and tapping (*right panel*)

$$\dot{x} = a_{01}y \quad \text{and} \quad \dot{y} = b_{ij}x^i y^j \quad \text{with } i + j \in [1, 3]. \quad (11)$$

3.6 Interpretation of the stochastic component

Figure 6b shows that this model fitting yields phase portraits that are very similar to the reconstructed ones in the case of forearm and wrist cycling (left and middle panels), supporting earlier studies of Kay et al. (1987, 1991) and Beek et al. (1996). For the tapping data, however, the results turn out to be quite poor because we ignored most prominent features like asymmetry and anchoring in constructing the model according to Eq. (9).

To account for these features, we repeated the model fit after including additional even terms in Eq. (9), that is, we formally substituted $i + j \in [0, 1, 2, 3]$ on the right-hand side. The resemblance between the resulting phase portrait (Fig. 7, left panel) and the numerically reconstructed phase portrait clearly improved. However, not only is the phase portrait still much smoother compared to the extracted dynamics, the vector field that corresponds to the fitted function (Fig. 7, right panel) does not display all anchoring effects that are present in the data. These rather local discrepancies hint at polynomial components of fairly high order because polynomials are known to converge quite slowly. The proper choice of functional forms covering all the features remains difficult. This problem illustrates how certain features of the movement may get lost in an inappropriate fit so that a direct comparison as shown above might be more appropriate.

For a two-dimensional system, the extracted stochastic component contains four numerical values at every point in phase space (i.e., at points at which an estimation was possible, see above). Hence, contrasting the analysis of the deterministic component, an immediate display by means of vector fields is no longer feasible. Gradisek et al. (2002a) combined the four extracted diffusion coefficients into individual 2×2 matrices and displayed them as geometrical objects located in the two-dimensional phase space lattice. This display allows for a local investigation of fluctuation strengths that we illustrate for the case of forearm cycling in Fig. 8. As geometrical objects we used ellipses whose diameters are given by the eigenvalues of the diffusion coefficient (2×2 matrix) and their inclination by the corresponding eigenvectors (note that Gradisek et al. 2002a, used parallelograms instead of ellipses). Since ellipses change shape when comparing peak positions and velocities with intermediate movement parts, we find that the noise strength depends on the cycling region. Put more formally, the fluctuations are signal dependent, which, in general, may be incorporated as multiplicative noise in the underlying dynamics. Interestingly, in this case the noise had little effects on zero and maximal velocity parts of the movement cycle.

To further analyse this signal dependent noise, we individually depicted the three different components of the diffusion coefficients (see Fig. 9). Recall that we computed

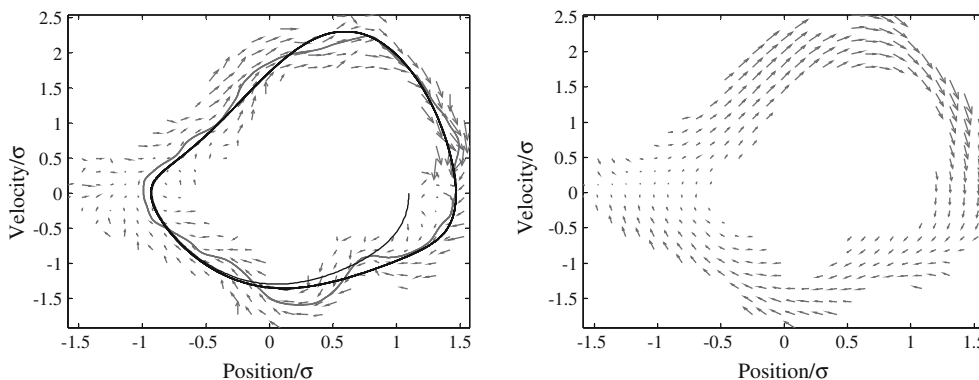


Fig. 7 *Left* Phase portrait (dark grey) generated by fitted function (Eq. 9 with $j \in [0,1,2,3]$) in addition to reconstructed phase portraits (light grey) and vector fields of tapping. *Right* Vector field generated by fitted function

four components; however, due to symmetry two of them turn out to be identical. Indeed these symmetric coefficients, the cross-terms $D_{xy}^{(2)}$, are rather weak when compared to the other components, suggesting that there is effectively no transfer of noise between variables. Because $D_{xx}^{(2)}$ and $D_{yy}^{(2)}$ are equally strong we suggest that the dynamic noise affects both position and velocity. As already discussed in Fig. 8, the noise strength depends on the location within the movement cycle. There, the noise strength appeared to have local minima at extreme positions and velocities, i.e., at four distinct regions in phase space. Figure 9, however, shows that $D_{xx}^{(2)}$ is ‘responsible’ for the minimal noise at the extreme positions whereas $D_{yy}^{(2)}$ ‘causes’ the minimal noise at the extreme velocities.

4 Discussion

In the present contribution we described a recently developed analysis approach for dynamical systems subject to both deterministic and stochastic influences. Building on its successful use in the treatment of problems in physics and related

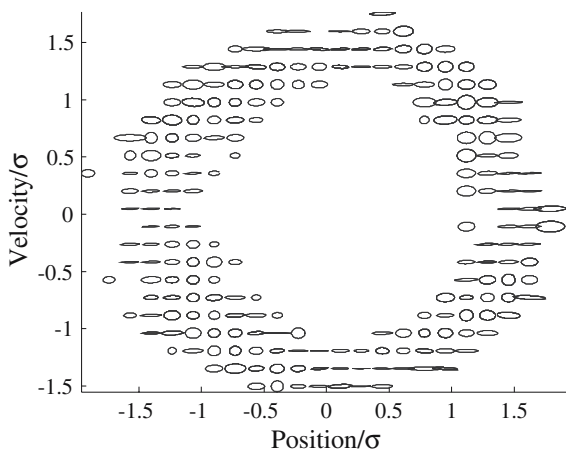


Fig. 8 Visualization of extracted noise coefficients from forearm cycling (movement tempo was 1.5 Hz); see text for explanation

fields, we explored its expedience in studying instances of rhythmic movement. Before speculating on the prospects of the analysis of deterministic and stochastic data components in general, we first recapitulate the illustrated merits of the approach in the study of human movement.

4.1 Analysis of human movement data

The dynamical system that is assumed to underlie recorded time series can be depicted by means of its corresponding vector field. In Figs. 5 and 6 we showed how extracted vector fields might be compared in terms of difference fields. This technique uncovers relative differences between the deterministic dynamics of, for instance, two movement conditions. Areas in phase space where marked differences occurred could be identified and interpreted in terms of their respective experimental constraints (e.g., flexion/extension differences, ‘discontinuities’ like in tapping and anchoring phenomena). Notice that the interpretations of the vector fields suggested here are by no means exhaustive; they merely served as easily accessible examples of the kind of information one might be able to glean from the extracted deterministic dynamics. Of course, this also applies to the interpretation of the stochastic component as illustrated in the context of the ellipse fields (as opposed to vector fields). In combination with the study of local effects of deterministic forms this may provide insight into the dynamical structure and the structure of noise as functions of location in phase space, also in relation to experimental conditions. Indeed, these functions are not prescribed, i.e., no additional assumptions regarding an appropriate analytical form are required. If desired, however, analytical functions can be mapped onto the extracted dynamics, e.g., to quantitatively compare findings with earlier studies. Then, vector fields like the ones depicted here can provide means to constrain the modeler’s intuition in choosing relevant analytical terms when seeking to reconstruct a particular dynamics. In particular, in the present analysis, particular dissipative terms (e.g., Rayleigh and van der Pol) were readily identified as deterministic components of a limit cycle description of smooth rhythmic movements in which iner-

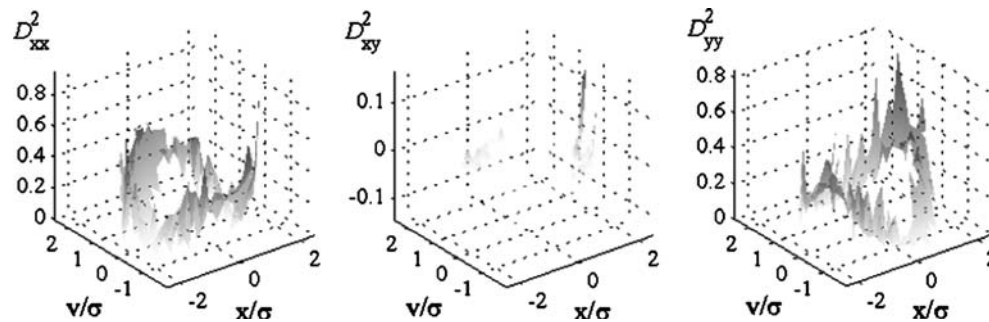


Fig. 9 Extracted diffusion coefficient, components depicted separately; see text for explanation

tia and impact forces played a marginal role, whereas higher order terms and more dimensions turned out to be indispensable in reconstructing the dynamical equations of motion for tapping. Difference fields between extracted and modeled dynamics may be of help in evaluating the quality of the derived models (e.g., tapping trajectories cannot be recovered by use of self-sustaining limit cycle oscillators with odd nonlinearities). In sum, the approach presented in this paper provides a solid, unbiased analysis tool for multidimensional dynamical systems consisting of deterministic and stochastic components. Unlike earlier approaches to extract ordinary differential equations for rhythmic movement like those of Beek and Beek (1988) and Eisenhammer et al. (1991), it does not require any a priori assumptions like finite polynomials, either for the drift or for the diffusion coefficient; furthermore, unlike those previously applied approaches, it is capable of extracting stochastic components.

4.2 Future prospects for analysis of deterministic structures in human movement

As explained above, the region in phase space where the dynamics can be extracted is confined to the area where data are present. In case of limit cycle behaviour like that of limb cycling movements, this region is typically restricted to the immediate vicinity of the (hypothetical) limit cycle. The ‘width of the vicinity’ is determined by the noise strength relative to the attractor strength and one may opt to increase noise in order to be able to cover a larger portion of the phase space in the analysis. However, considering that the structured manipulation of the noise strength can be difficult (e.g., Breeden et al. 1990), we suggest exploiting the transient behaviour of a dynamics rather than trying to add random perturbations. For instance, imposing distinct initial conditions from where the system starts relaxing towards its stable regime may allow for scanning dynamical properties at locations that will never be visited in steady-state behaviour. The trial-for-trial variation of initial transients in combination with the averaging of extracted transition probabilities is thus a means to scan the dynamics throughout the phase space.

4.3 Future prospects for analysis of stochasticity in human movement

van Beers et al. (2004) discerned three processes in which noise arises that may contribute to movement variability: target localization, movement planning and movement execution. These three stages may be subdivided into substages. For example, movement execution may be investigated at various levels, including neural signals, muscle activation, kinematic profiles and task performance. At all these levels variability is present to some degree. Contrary to the assumption of van Beers et al. (2002) that the central nervous system organizes movements in order to minimize the ‘detrimental effects’ of all these noise sources, it appears that the variability has functional qualities (see introduction). In the study of human movement, numerous efforts have been made to identify the origin and form of variability at all these levels. Because of the diversity of levels of investigation, interpretations of variability and (single) quantitative measures used, the chances of such studies amalgamating are slim at best. With the extraction procedure presented here, the stochastic element of human movement can be extracted and analysed in an unbiased way. The fact that it produces not a single but a phase space-dependent measure allows for much more detailed investigations of variability. Moreover, the effects of noise contribution in, for example, target localization versus movement planning versus movement execution could be discerned by tuning experimental conditions in such a way that these effects can be separated (van Beers et al. 2004) and their relative contributions compared by means of the extracted stochastic component. Likewise, the effects of measurement noise (i.e., noise due to experimental measurement devices) versus dynamical noise (i.e., noise inherent to the system under study) could be addressed as suggested by Siefert et al. (2003) and Frank et al. (2004).

5 Conclusion

The main advantage of the analysis explained here over conventional approaches is that the separation of the dynamics into Kramers–Moyal coefficients allows for detailed studies of deterministic and stochastic parts in dynamical systems

with noise. The method does not require any assumptions regarding possible analytical forms of the underlying, generating dynamics and can thus be viewed as an entirely unbiased tool. Furthermore, not only the steady-state but also transient behavior can be invoked which may actually improve numerical estimates by increasing the phase space area that is accessible for analysis.

Appendix

A Multidimensional forms

We reformulate the earlier introduced mathematical forms by means of n -dimensional dynamical systems (boldface characters represent vectors, matrices or tensors). For an n -dimensional system the Fokker–Planck operator in Eq. (1) has the form

$$L_{FP} = -\nabla_x \left\{ D^{(1)}(x) - \nabla_x D^{(2)}(x) \right\},$$

where ∇_x denotes the gradient operator with respect to state variables \mathbf{x} . Accordingly, the Fokker–Planck equation becomes:

$$\frac{\partial}{\partial t} P(x, t) = -\nabla_x \left\{ D^{(1)}(x) - \nabla_x D^{(2)}(x) \right\} P(x, t)$$

with Kramers–Moyal coefficients:

$$D^{(n)}(x) = \lim_{\tau \rightarrow 0} \frac{1}{\tau} \int \frac{[x' - x]^n}{n!} P(x', t + \tau | x, t) dx'$$

In view of the Pawula theorem, i.e., if $D^{(n=4)}(x) = 0$ holds and, thus, all cumulants of order three and higher vanish, the corresponding dynamical system describes a Gauss diffusion process by means of the (Stratonovich-)Langevin equation:

$$\frac{d}{dt} \xi = D^{(1)}(\xi) + \left[2D^{(2)}(\xi) \right]^{1/2} \cdot \Gamma[t].$$

B Markov properties and the Chapman–Kolmogorov test

The sketched approach requires the system to be a Markov process. We denote the system's state variables by \mathbf{x} and $P(\mathbf{x}', t' | \mathbf{x}, t)$ is the probability density to find the system at time t' at state \mathbf{x}' presuming the previous state \mathbf{x} at time t ($t'' \geq t' \geq t$). Then we can test for Markov properties by verifying the integral Chapman–Kolmogorov equation:

$$P(\mathbf{x}'', t'' | \mathbf{x}, t) = \int \underbrace{P(\mathbf{x}'', t'' | \mathbf{x}', t') P(\mathbf{x}', t' | \mathbf{x}, t)}_{=\tilde{P}(\mathbf{x}'', t'' | \mathbf{x}, t)} dx'$$

That is, we calculate conditional probabilities for the time differences $t'' - t$, $t'' - t'$, etc., and compare the resulting two distributions in terms of, for instance, a conventional χ^2 -statistics (Press et al. 1994, chapter 14.3, page 622):

$$\chi^2 = \int \int \frac{\left[P(\mathbf{x}'', t'' | \mathbf{x}, t) - \tilde{P}(\mathbf{x}'', t'' | \mathbf{x}, t) \right]^2}{P(\mathbf{x}'', t'' | \mathbf{x}, t) + \tilde{P}(\mathbf{x}'', t'' | \mathbf{x}, t)} dx'' dx.$$

References

- Beek PJ, Beek WJ (1988) Tools for constructing dynamical models of cyclical movement. *Hum Mov Sci* 7:301–342
- Beek PJ, Peper CE, Stegeman DF (1995) Dynamical models of movement coordination. *Hum Mov Sci* 14: 573–608
- Beek PJ, Rikkert WEI, van Wieringen PCW (1996) Limit cycle properties of cyclical forearm movements. *J Exp Psychol Hum Percept Perform* 22:1077–1093
- van den Berg C, Beek PJ, Wagenaar RC, van Wieringen PCW (2000) Coordination disorders in patients with Parkinson's disease: a study of paced rhythmic forearm movements. *Exp Brain Res* 134:174–186
- Beek PJ, Peper CE, Daffertshofer A (2002) Modeling rhythmic interlimb coordination: beyond the haken–kelso–bunz model. *Brain Cogn* 48:149–165
- van Beers RJ, Baraduc P, Wolpert DM (2002) The role of uncertainty in sensorimotor control. *Philos Trans R Soc Lond B Biol Sci* 357:1137–1145
- van Beers RJ, Haggard P, Wolpert DM (2004) The role of execution noise in movement variability. *J Neurophysiol* 91:1050–1063
- Bootsma RJ, Mottet D, Zaai FTJM (1998) Trajectory formation and speed-accuracy trade-off in aiming movements. *Life Sci* 321:377–383
- Breeden JL, Dinkelacker F, Hübner A (1990) Noise in the modeling and control of dynamical systems. *Phys Rev A* 42:5827–5836
- Eisenhammer T, Hübner A, Packard N, Kelso JAS (1991) Modeling experimental time series with ordinary differential equations. *Biol Cybern* 65:107–112
- Frank TD, Daffertshofer A, Beek PJ (2001) Multivariate ornstein-uhlenbeck processes with mean-field dependent coefficients: application to postural sway. *Phys Rev E* 63:011905
- Frank TD, Beek PJ, Friedrich R (2004) Identifying noise sources of time-delayed feedback systems. *Phys Lett A* 328:219–224
- Friedrich R, Peinke J (1997) Description of a turbulent cascade by a fokker-planck equation. *Phys Rev Lett* 78:863–866
- Friedrich R, Peinke J, Renner C (1997) How to quantify deterministic and random influences on the statistics of the foreign exchange market. *Phys Rev Lett* 84:5224–5227
- Friedrich R, Siegert S, Peinke J, Lück St, Siefert M, Lindemann M, Raethjen J, Deuschl G, Pfister G (2000) Extracting model equations from experimental data. *Phys Lett A* 271:217–222
- Gardiner CW (2004) *Handbook of stochastic methods*. Springer series in synergetics, vol 13, 3rd edn. Springer, Berlin Heidelberg New York
- Gradisek J, Siegert S, Friedrich R, Grabec I (2000) Analysis of time series from stochastic processes. *Phys Rev E* 62:3146–3155
- Gradisek J, Govekar E, Grabec I (2002a) Qualitative and quantitative analysis of stochastic processes based on measured data II: applications to experimental data. *J Sound Vib* 252:563–572
- Gradisek J, Grabec I, Siegert S, Friedrich R (2002b) Qualitative and quantitative analysis of stochastic processes based on measured data I: theory and application to synthetic data. *J Sound Vib* 252:545–562
- Haken H (1983) *Synergetics*. Springer, Berlin Heidelberg New York
- Haken H, Kelso JAS, Bunz HA (1985) Theoretical model of phase transitions in human hand movements. *Biol Cybern* 51:347–356
- Harris CM, Wolpert DM (1998) Signal-dependent noise determines motor planning. *Nature* 394:780–784
- Honerkamp J (1998) *Statistical physics*. Springer, Berlin Heidelberg New York
- Kay BA (1988) The dimensionality of movement trajectories and the degrees of freedom problem: a tutorial. *Hum Mov Sci* 7:343–364
- Kay BA, Kelso JAS, Saltzman EL, Schöner G (1987) The space-time behavior of single and bimanual rhythmic movements: data and model. *J Exp Psychol Hum Percept Perform* 13:178–192
- Kay BA, Kelso JAS, Saltzman EL (1991) Steady-state and perturbed cyclical movements: a dynamical analysis. *J Exp Psychol Hum Percept Perform* 17:183–197
- Kelso JAS (1984) Phase-transitions and critical-behavior in human bimanual coordination. *Am J Physiol* 246:1000–1004
- Körding KP, Wolpert DM (2004) Bayesian integration in sensorimotor learning. *Nature* 427:244–247

- Kramers HA (1940) Brownian motion in a field of force and the diffusion model of chemical reaction. *Physica* 7:284–304
- Kriso S, Peinke J, Friedrich R, Wagner P (2002) Reconstruction of dynamical equations of traffic flow. *Phys Lett A* 299:287–291
- Kuusela T, Shepherd T, Hietarinta J (2003) Stochastic model for heart-rate fluctuations. *Phys Rev E* 67:061904
- Mottet D, Bootsma RJ (1999) The dynamics of goal-directed cyclical aiming. *Biol Cybern* 80:235–245
- van Mourik AM, Daffertshofer A, Beek PJ (2005) Extraction of Kramers–Moyal coefficients from short and non-stationary data sets. *Phys Lett A* (in press), PLA 15063
- Moyal JE (1949) Stochastic process & statistical physics. *J R Stat Soc (Lond) B* 11:150
- Perona P, Porporato A, Ridolfi L (2000) On the trajectory method for the reconstruction of differential equations from time series. *Nonlin Dyn* 23:13–33
- Post AA, Peper CE, Daffertshofer A, Beek PJ (2000) Relative phase dynamics in perturbed interlimb coordination: stability and stochasticity. *Biol Cybern* 83:443–459
- Press WH, Teukolsky SA, Vetterling W, Flannery BP (1994) Numerical recipes in C: the art of scientific computing, 2nd edn. Cambridge University Press, Cambridge
- Riley MA, Turvey MT (2002) Variability and determinism in motor behaviour. *J Mot Behav* 34:99–125
- Risken H (1989) The Fokker–Planck equation. Springer, Berlin Heidelberg New York
- Siefert M, Kittel A, Friedrich R, Peinke J (2003) On a quantitative method to analyze dynamical and measurement noise. *Europhys Lett* 61:466–472
- Siebert S, Friedrich R, Peinke J (1998) Analysis of data sets of stochastic systems. *Phys Lett A* 243:275–280
- Schöner G, Haken H, Kelso JAS (1986) A stochastic theory of phase transitions in human hand movement. *Biol Cybern* 53:247–257
- Schöner G (1990) A dynamic theory of coordination of discrete movement. *Biol Cybern* 63:257–270
- Schöner G (2002) Timing, clocks and dynamical systems. *Brain Cogn* 48:31–51
- Stratonovich R (1963) Topics in the theory of random noise, vol I&II. Gordon and Breach, New York
- Sura P (2003) Stochastic analysis of southern and pacific ocean sea surface winds. *J Atmos Sci* 60:654–666
- Todorov E, Jordan MI (2002) Optimal feedback control as a theory of motor coordination. *Nat Neurosci* 5:1226–1235
- Waechter W, Riess F, Kantz H, Peinke J (2003) Stochastic analysis of surface roughness. *Europhys Lett* 64:579–585